Article

The Effect of Slag on the Mechanical Properties of Coralline-Activated Materials and the Formation and Transformation of Mineral Crystals

Guodong Huang [1,2,3,4,*], Jielei Zhu [1,3], Yuting Zhang [1,3], Dawei Li [1], Bo Wang [1], Mengrong Li [1], Lina Jin [5] and Jinghai Gong [5]

1   School of Civil Engineering and Construction, Anhui University of Science and Technology, Huainan 232001, China; jlzhu@aust.edu.cn (J.Z.); ytzhang@aust.edu.cn (Y.Z.); dwli@aust.edu.cn (D.L.); bowang@aust.edu.cn (B.W.); mrli@aust.edu.cn (M.L.)
2   Hefei Comprehensive National Science Center, Institute of Energy, Hefei 230031, China
3   Institute of Environment-Friendly Materials and Occupational Health, Anhui University of Science and Technology, Wuhu 241003, China
4   Engineering Quality Inspection and Safety Evaluation, Fujian University Engineering Research Center, Longyan 364000, China
5   Jiangsu Lanquan New Material Inc., Ltd., Zhenjiang 212000, China; sales@jslanquan.com (L.J.); brjxcl@163.com (J.G.)
*   Correspondence: gdhuang@aust.edu.cn

Abstract: In this study, coralline-activated materials were prepared using ball-milled coral powder as cementitious material and coral sand as fine aggregate. XRF (X-ray fluorescence) and chemical dissolution tests were carried out to determine the content and reactivity of various elements in coral powder. The compressive strength of the developed composites was evaluated at different ages, and the formation and transformation of mineral crystals in coralline-activated samples were further analyzed by XRD (X-ray diffractometer). The results show that the calcium content in coral powder was as high as 89.5% (loss on ignition). However, only 56% of the active calcium could participate in the polymerization reaction. The silicon and aluminum content was too low, and the slag addition could improve the deficiency of silicon and aluminum in coral powder. With the increase in slag content (from 0% to 50%), the compressive strength of the composites increases significantly. Nevertheless, the enhancement is not pronounced when the slag content exceeds 50%. The increase in slag amount can stimulate the transformation of calcium minerals, e.g., aragonite and calcite, into hydrated calcium silicate and calcium aluminosilicate gels, which significantly enhances the resulting compressive strength.

Keywords: alkali-activated materials; coral powder; active calcium and silicon; crystal; compressive strength

1. Introduction

In order to develop the ocean economy and safeguard the strategic deployment of maritime rights and interests, China is gradually accelerating the construction of hydraulic reclamation of ocean islands and reefs. However, the hydraulic reclamation of ocean islands and reefs is quite complex. It poses several technical issues, among which the foremost is to solve the problem of the source of hydraulic fill materials [1]. The transportation of raw materials for concrete, such as cement, sand, and gravel, from inland for hydraulic fill construction significantly increases the construction cost and severely affects the construction cost, period, and quality [2]. Mixing coral with seawater to prepare concrete for the hydraulic reclamation of islands and reefs effectively solves such challenges [3]. Many researchers have conducted extensive and in-depth studies on the properties of coral concrete [4]. Therefore, coral concrete has gradually become the main building material for

island and reef construction because of its intrinsic characteristics and advantages, such as convenient materials availability, environmental protection, and economy [5].

However, many detailed investigations on the coral concrete properties have revealed several shortcomings in its workability, mechanical properties, and durability [6]. First, the use of coral concrete only solves the problem of the aggregate source; however, the cementitious materials required for concrete still need to be transported from inland for a long distance. Second, compared to the conventional coarse aggregates, coral aggregate has inferior quality due to inherent defects, such as multiple interior pores and irregular shape. It results in significantly increased mixing water demand, thereby reducing the resulting mechanical properties of coral concrete and significantly increasing the difficulty of mixing and pouring coral concrete [7]. Moreover, corals are mainly formed by calcium carbonate deposition. The crushed stone used to prepare concrete is formed by igneous rocks through complex geological changes, leading to the lower strength of coral aggregate than crushed stone [8]. Therefore, high-strength cement mortar is used to wrap low-strength coral aggregate, thus, forming weak pockets in the strong cementitious matrix [9]. Thus, when the coral aggregate is fractured in the concrete, the cement mortar is far from reaching the fracture strength. This approach is neither economic nor scientific, and the coral aggregate must be modified and strengthened before application [10]. Finally, the strength development of calcium silicate hydrate (C-S-H) gel formed by cement hydration is slow, leading to low early strength development of coral concrete, which causes the settlement of coral concrete after completion. It severely affects the filling effect.

In order to overcome the limitations of coral concrete in material performance, in this study, a kind of coral alkali-activated hydraulic fill material was developed by alkali activation [11]. Alkali-activated materials are a new type of cementitious material that, through strong alkali reactions with silicate or aluminosilicate minerals, form hydrated calcium silicate or hydrated calcium aluminosilicate gels by polymerization [12]. More importantly, unlike the conventional cement-based materials, alkali-activated materials have the properties of quick setting, rapid early strength development, and high strength at the later stage (after 28 d of curing) [13,14]. Thus, ball-milled coral powder was used as the cementitious material, while coral sand was used as fine aggregates to prepare coral alkali-activated hydraulic fill material. In this way, a low-cost composite using local materials can be achieved for hydraulic reclamation, significantly reducing the construction cost and period.

However, to obtain coralline alkali-activated materials with excellent performance, it is critical to deeply analyze the mineralogical composition and reactivity of corals and enhance the polymerization through appropriate mineral admixtures [15]. Therefore, in this paper, XRD and XRF are first used to determine the chemical and mineral composition of coral. The reactivity of various substances in coral is also analyzed through chemical dissolution experiments. The content of active calcium, silicon, and aluminum in raw materials was adjusted by adding different proportions of ground granulated blast furnace slag and coral powder. The compressive strength development of the samples was determined at different ages, and the corresponding trend was studied. The formation and transformation of mineral crystals in coralline-activated materials and their influence on strength development were analyzed by XRD. Lastly, coralline-activated materials with excellent properties were prepared.

2. Materials and Methods

2.1. Materials

2.1.1. Coral Powder and Granulated Blast Furnace Slag Powder

Coral powder (CP) and granulated blast furnace slag powder (GSP) were used as binders to prepare alkali-activated materials. CP (Xiangtai mineral products Co., Ltd., Shijiazhuang, Hebei, China) was made from coral stone by drying and ball milling. First, the coral stone was placed in the oven and dried continuously at 60 °C for 3 h. Subsequently, the coral stone was placed in a ball mill for continuous ball milling for 30 min. The surface

area of CP was greater than 300 m^2/kg, and the particle fineness reaching the margin of a square-hole sieve (45 µm) was less than 26%. The chemical of CP obtained from X-ray fluorescence spectroscopic analysis (XRF) is shown in Table 1. GSP is mainly used as active silicon and aluminum-increasing agent. The specific surface area of GSP was 400 m^2/kg, and the particle fineness reaching the margin of the square-hole sieve (45 µm) was less than 16%. Its chemical is also listed in Table 1.

Table 1. Chemical composition (%).

	SiO$_2$	Al$_2$O$_3$	Fe$_2$O$_3$	CaO	MgO	Na$_2$O	K$_2$O	Others	Loss
CP	1.7	0.3	0.2	50.7	0.8	-	-	2.7	43.3
GSP	31.4	18.7	0.6	34.7	9.3	1.3	0.8	2.3	0.73

2.1.2. Sodium Hydroxide and Liquid Sodium Silicate

Sodium hydroxide (NaOH) was used as the activator, establishing a highly alkaline excitation environment for polymerization. NaOH is an analytical reagent. The liquid sodium silicate (Na$_2$SiO$_3$) used in this work was industrial grade with purity greater than 95%, with Na$_2$O, SiO$_2$, and H$_2$O as 9.68%, 25.26%, and 65.02% of the total mass, respectively.

2.1.3. Other Materials

The fineness modulus of coral sand used in this study is 1.65, and seawater is used for mixing and preparing the composite.

2.2. *Sample Preparation*
2.2.1. Mix Proportions of the Samples

The mix proportions of CP alkali-activated samples are shown in Table 2. Sample H-1 only uses CP to prepare alkali-activated samples, to test the polymerization performance of CP, and is taken as the control group. From samples H-2 to H-10, the GPS content was increased (increase by 10% each level), while the CP content was reduced in the same proportion. The ratio of active calcium, silicon and aluminum in CP was adjusted through the GPS content to achieve the best mechanical properties.

Table 2. Mix proportion of the samples/g.

	CP	GSP	Water	Liquid Sodium Silicate	NaOH	Sand	L/S
H-1	450	/	147	120	20	1350	0.5
H-2	/	450	147	120	20	1350	0.5
H-3	405	45	147	120	20	1350	0.5
H-4	360	90	147	120	20	1350	0.5
H-5	315	135	147	120	20	1350	0.5
H-6	270	180	147	120	20	1350	0.5
H-7	225	225	147	120	20	1350	0.5
H-8	180	270	147	120	20	1350	0.5
H-9	135	315	147	120	20	1350	0.5
H-10	90	360	147	120	20	1350	0.5

2.2.2. Sample Preparation and Curing

The preparation method of CP alkali-activated samples is described as follows. First, NaOH was dissolved in the test water according to the proportions presented in Table 2. Then, CP and GSP were placed into the mixer and mixed evenly. NaOH solution was added and stirred quickly for 45 s; then, coral sand and liquid sodium silicate were added and stirred quickly for 45 s. The mixed alkali-activated mortar was cast into 40 × 40 × 160 mm molds for compressive strength testing. The prepared mortars were placed in a curing chamber at 20 ± 2 °C above 95% humidity. After 24 h curing, the specimens were removed from the molds and remained in the curing chamber until the testing age.

2.3. Experimental Methods

2.3.1. Determination of Active Substance Content and Reaction Activity

First, the composition and content of chemical substances in raw materials (CP and GSP) were analyzed by XRF. Then, the reaction activity in raw materials was further determined by chemical dissolution experiments as per the "method for the chemical analysis of cement" GB/T176-2017 [16].

The reaction activity test is divided into four procedural steps.

(1) Acid dissolution: 10 g sample (CP or GSP) was dissolved in 100 mL hydrochloric acid with a concentration of 1 mol/L and mixed evenly. The mixture was heated in boiling water for 15 min and then filtered. The filtered residue was obtained via alkali dissolution.

(2) Alkali dissolution: The filtered residue was dissolved in 100 mL NaOH solution with a 1 mol/L concentration and stirred evenly. It was then placed in boiling water for 15 min, and the insoluble residue was filtered out.

(3) Drying and determination: The insoluble residue was calcined in a muffle furnace at 1000 °C for 30 min. After calcination, residual solid mass was measured, and the contents of chemical components were analyzed again via XRF. The insoluble substance is used as the inert substance without polymerization activity.

(4) Calcination: The mass loss after the chemical dissolution was used as the reactive activity and was calculated from Equation (1).

$$Pr = (Mt \times P\omega - Mr \times P\omega)/Mt \tag{1}$$

where Pr represents the proportion of active chemical composition, Mt represents the total mass before reaction, Mr represents the mass of the residue after the reaction, and $P\omega$ represents the proportion of the chemical composition.

2.3.2. Compressive Strength Test

A TYE-300 automatic press was used to test the compressive strength of PC alkali-activated mortars cured for 3, 28, and 60 days. The final results were obtained by averaging the results from six different tests.

2.3.3. XRD Measurements

The paste samples cured for 28 d were investigated through XRD. SmartLab SE intelligent X-ray diffractometer was used to determine the characteristics of micro-mineral crystals in CP alkali-activated materials. The effects of different proportions of GPS on the formation and transformation of mineral crystals in CP alkali-activated samples were evaluated. Further, the XRD results were combined with the compressive strength data to analyze the relationship between the compressive strength development and the crystal formation and transformation in CP alkali-activated materials.

3. Results and Discussions

3.1. Chemical Composition and Reactivity Analysis

(1) Chemical composition analysis of raw materials

The XRF analysis showed that CP is primarily composed of calcium, accounting for 50.7% of the total. At the same time, it also contains trace elements such as silicon, aluminum, and iron, amounting for merely 5.7% of the total. However, the loss on ignition of CP is as high as 43.3%, which is due to calcium carbonate decomposition in CP at high temperatures. Therefore, CP is a typical material with high calcium and low silicon and aluminum content, since alkali-activated materials are mainly polymerized by active substances such as calcium, silicon, and aluminum to form polymerization products such as hydrated calcium silicate and hydrated calcium silico-aluminate gels [17]. Although the high calcium content in CP plays a significant role in promoting the formation of polymerization products, the low silicon and aluminum contents in CP are unfavorable to

the formation of hydrated calcium silicate and hydrated calcium silicoaluminate. Therefore, it is not suitable to be used as the raw material of alkali-activated material alone, only by adding other mineral additives to modify the CP to increase silicon and aluminum.

Meanwhile, the XRF analysis of GSP shows that it is mainly composed of calcium, silicon, aluminum, and magnesium, accounting for 34.7%, 31.4%,18.7%, and 9.3%, respectively. Other elements such as iron, sodium, and potassium account for only 5% of the total. Compared with the chemical composition of CP, the contents of active calcium, silicon, and aluminum in GSP are more balanced. Therefore, GSP can be added to CP to improve the content of active silicon and aluminum, modify and activate CP, and make it suitable for use as the raw material of alkali-activated material [18].

(2) Chemical composition reactivity analysis

Table 3 shows the analysis results of the chemical dissolution experiments of CP and GSP. Regarding the quality change analysis, since the loss on ignition of CP is as high as 43.3%, after removing the loss on ignition, the actual mass of CP is only 5.67 g. After the chemical dissolution test, the insoluble residue in CP reaches up to 3.5 g, accounting for 61.7% of the total mass. The mass of dissolved substances only reaches 2.17 g, accounting for 38.3% of the total mass. It indicates that only 38.3% of the components in CP is active and can be dissolved and participate in the polymerization reaction. In comparison, 61.7% of CP is completely inert, which only serves as the filling in the alkali-activated material. The content of active substances in CP is noticeably insufficient, which severely affects the mechanical properties of CP alkali-activated samples.

Table 3. Reactivity of CP/GSP determined by chemical dissolution and XRF (wt %).

		SiO_2	CaO	Al_2O_3
I H-1/H-2 CP/GSP	10 g(5.67 g)/10 g	2.9/31.4	89.5/34.7	0.5/18.7
II Residue	3.5 g (61.7%)/0.8 g (8%)	2.5/55.3	95.6/23.4	0.2/6.1
III Active components	2.17 g (38.3%)/9.2 g (92%)	2.0/27.0	56.0/32.8	0.4/18.2
VI Dissolution rate		69/86.0	62.6/94.5	99/97.3
H-3 90%CP + 10%GSP		4.5/70.7	53.7/65.8	2.2/98.8
H-4 80%CP + 20%GSP		7.0/72.4	51.4/69.0	4.0/98.7
H-5 70%CP + 30%GSP		9.5/74.1	49.0/72.2	5.7/98.5
H-6 60%CP + 40%GSP	Active components	12.0/75.8	46.7/75.4	7.5/98.3
H-7 50%CP + 50%GSP	/Dissolution rate	14.5/77.5	44.4/78.6	9.3/98.2
H-8 40%CP + 60%GSP		17.0/79.2	42.1/81.7	11.1/98.0
H-9 30%CP + 70%GSP		19.5/80.9	39.8/85.0	12.9/97.8
H-10 20%CP + 80%GSP		22/82.6	37.4/88.1	14.6/97.6

(CP: III = I − II × 35%; GSP: III = I − II × 8%, VI = III/I; GBFS: III = I − II × 14.32%, VI = III/I).

Regarding the analysis from element change, before the dissolution test, the contents of calcium, silicon, and aluminum in CP reach 89.5%, 2.9%, and 0.5%, respectively. However, after the dissolution tests, the contents of insoluble calcium, silicon, and aluminum in CP residue reach up to 95.6%, 2.5%, and 0.2%, respectively, indicating that the insoluble matter is mainly composed of calcium. Moreover, because a large amount of calcium is insoluble, although the calcium content in CP is as high as 89.5%, the active calcium content accounts for only 56%, i.e., almost half of the calcium in CP is inert. Therefore, the deficiency of active calcium content and low dissolution rate will further affect the polymerization activity of CP and adversely affect the mechanical properties of CP alkali-activated samples.

Regarding the quality change analysis of GSP, after the dissolution test, the insoluble matter in GSP is only 1.2 g, accounting for 12% of the total mass. The soluble matter is as high as 8.8g, accounting for 88% of the total mass. Regarding the analysis from element change, before the dissolution test, the contents of calcium, silicon, and aluminum in GSP are 34.7%, 31.4%, and 18.7%, respectively. After the dissolution test, active calcium, silicon, and aluminum contents are 32.8%, 27%, and 18.2%, respectively, and the dissolution rates are as high as 94.5%, 86%, and 97.3%. Compared with CP, the proportion of calcium,

silicon, and aluminum in GSP is more balanced, and the proportion of active components is significantly higher than CP. More importantly, the dissolution rate of active components is also significantly higher than CP. Therefore, the polymerization activity of GSP is better than CP. The modification and enhancement of CP can be achieved by adding GSP into CP [19].

(3) Enhancement effect of GSP on CP

The effect of GSP on improving CP is shown in Table 3. When mixing 10% GSP into 90% CP, the active silicon content in sample H-3 increased to 4.5%, which was significantly higher than pure CP (2%). In addition, the dissolution rate increased to 70.7%, which is slightly higher than pure CP (69%). With the increase in GSP incorporation ratio, the content and dissolution rate of active silicon continued to increase. When mixing 80% GSP into 20% CP, the active silicon content in sample H-10 increased to 22.0%, and the dissolution rate also increased to 82.6%. A severe lack of active silicon in CP makes it only rich in calcium, prevents it from carrying out polymerization, and inhibits the formation of hydrated calcium silicate and hydrated calcium aluminosilicate gels. Therefore, incorporating GSP can significantly increase the content and the dissolution rate of active silicon, creating favorable conditions for the formation of polymerization products, which are favorable to the compressive strength development of the resulting composite [20,21].

For active calcium, when mixing 10% GSP into 90% CP, the active calcium content in sample H-3 decreased to 53.7% instead and was slightly lower than pure CP (56%). However, the dissolution rate of active calcium increased to 65.8%, which was slightly higher than pure CP (62.6%). With the increase in GSP content, the content of active calcium continued to decrease slowly, while the dissolution rate of active calcium continued to increase. When the content of GSP reaches 80%, the content of active calcium in sample H-10 decreases to 37.4% but the dissolution rate increases to 88.1%. However, the calcium content in only CP has been as high as 89.5%. However, the dissolution rate is only 62.6%, which hinders the efficiency of active calcium participating in polymerization and delays the formation of polymerization products. Although the substitution of CP by GSP slightly reduces the content of active calcium in samples, it significantly improves the dissolution rate of active calcium. Moreover, the amount of active calcium participating in the polymerization reaction can be compensated by the increase in dissolution rate; thus, it will not adversely affect the polymerization rate and the formation of polymerization products [22].

For active aluminum, when mixing 10% GSP into 90% CP, the active aluminum content in sample H-3 increased to 2.2%, which was significantly higher than pure CP (0.4%). Further, the dissolution rate of active aluminum in the mixture remained at 98.8%, which was not substantially lower than pure CP (99%). With the gradual increase in GSP content, the content of active aluminum in samples increases continuously, and the dissolution rate of active aluminum decreases slowly. When the content of GSP reaches 90%, the content of active aluminum in sample H-10 increases to 14.6%, and the dissolution rate decreases to 97.6%. Active aluminum is an important part of hydrated calcium silicoaluminate in the polymerization product of alkali-activated materials. However, the lack of active aluminum content in CP will seriously restrict the formation of hydrated calcium silicoaluminate, which hinders the compressive strength development. Therefore, the addition of GSP can significantly improve the defect of serious deficiency of active aluminum content in CP and will not adversely affect the dissolution rate of active aluminum [23].

3.2. Compressive Strength Analysis

3.2.1. Pure CP and GPS Alkali-Activated Samples

The compressive strength of alkali-activated samples is shown in Figure 1. The compressive strength of sample H-1 (the control specimen group) only reaches 1.2 MPa after curing for 3 days. When the curing age increases to 28 and 60 d, the compressive strength only increases to 3.7 and 4.2 Mpa, respectively. The compressive strength of sample H-1 is inferior and does not increase significantly with curing age. From the

chemical composition and reactivity analyses of CP (Section 3.1), it is inferred that due to the lack of active silicon and aluminum required for polymerization products in CP, it is impossible to form calcium silicate hydrate and hydrated calcium aluminosilicate gel in sample H-1. It also confirms that even CP with high calcium cannot form excellent mechanical properties without silicon and aluminum.
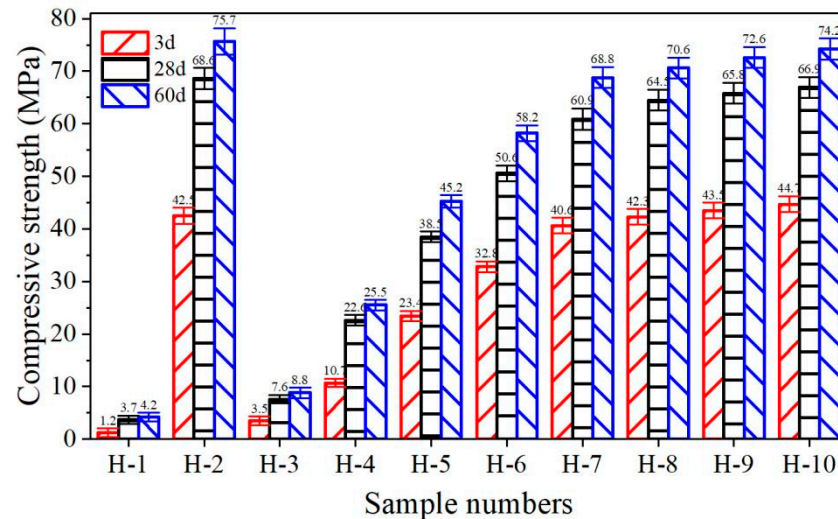

Figure 1. Compressive strength of polymer samples.

When pure GPS is used to prepare alkali-activated samples (i.e., H-2), the compressive strength increases rapidly to 42.5 MPa after curing for 3 days. When the curing age increases to 28 and 60 d, the compressive strength increases to 68.6 and 75.7 MPa, respectively. The growth trend of compressive strength in sample H-2 is obvious and completely different from sample H-1. The content of active calcium in GPS is lower than CP. GPS also contains large amounts of active silicon and aluminum. The content distribution is more balanced (Table 1), which creates a good scenario for forming high-strength polymerization products [24]. This is the main reason for the high compressive strength in sample H-2.

3.2.2. Analysis of GPS Modified CP

When 10% GPS is incorporated, the compressive strength of sample H-3 cured for 3 d increases to 3.5 MPa, and it further increases to 7.6 and 8.8 MPa when curing for 28 and 60 d. GPS addition can improve the compressive strength of sample H-3, but the enhancement effect is not much pronounced. GPS incorporation provides active silicon and aluminum for a polymerization reaction environment, promoting the formation of polymerization products, thereby improving the resulting compressive strength [25]. However, since the amount of GPS is merely 10%, the amount of active silicon and aluminum introduced is insufficient. Thus, a large amount of active calcium still cannot be polymerized; thus, the increase in compressive strength is not obvious.

When the content of GPS increased to 20% (sample H-4), the compressive strength of specimens cured for 3 d increased to 10.7 MPa, which further increased to 22.6 and 25.5 MPa when curing was prolonged to 28 and 60 d, respectively. With the increase in GPS content, the growth rate of compressive strength in sample H-4 began to increase significantly. In addition, with the increase in GPS content, the growth rate of compressive strength in samples H-5 and H-6 was still obvious. Before reaching the GPS content of 50%, the compressive strength of sample H-7 cured for 3 d increased to 40.6 MPa, which further increased to 60.9 and 68.8 MPa when curing for 28 and 60 d, respectively; it was only 4.5%, 11.2%, and 10% lower than sample H-2 (100% GPS) for the corresponding curing ages. It indicates that increasing the GPS amount improves active silicon and aluminum in the mix and makes the excess active calcium continue to polymerize with active silicon and

aluminum; it increases the polymerization rate and improves the formation of high-strength polymer products to achieve the goal of improved mechanical strength [26].

However, when the GPS content exceeds 50%, the compressive strength enhancement effect starts fading away quickly. When the GPS content is up to 60%, the compressive strength of sample H-8 cured for 3 d only increased to 42.3 MPa and increased to 64.5 and 70.6 MPa when curing for 28 and 60 d, respectively, which is merely 4.2%, 5.9%, and 2.6% higher than sample H-7 (50% GPS). Even when the content of GPS was up to 80%, the compressive strength of sample H-10 cured for 3 d only increased to 44.7 MPa and increased to 66.9 and 74.2 MPa when curing for 28 and 60 d, respectively, which is only 5.7%, 3.7%, and 5.1% higher than sample H-8 (60% GPS). When the content of GPS exceeds 50%, the enhancement effect begins to decrease significantly. This is mainly because the formation of polymerization products requires an adequate amount of calcium, silicon, and aluminum. A GPS amount higher than 50% leads to the excess of active silicon and aluminum in the polymerization environment and the lack of active calcium to participate in the polymerization reaction, which also affects the formation of polymerization products [27]. This is why the compressive strength of H-7 to H-10 does not increase significantly when the GPS content surpasses 50%.

3.3. XRD Analysis

3.3.1. XRD Analysis of the Raw Materials

(1) XRD analysis of GPS

The XRD analysis of raw materials is shown in Figure 2. No obvious characteristic crystal peaks appearing in GPS could be seen. Only a low steamed bread peak appears near 30 degrees (2-theta), indicating that GPS contains a greater amount of amorphous calcium and silicon. GPS is a by-product produced by smelting pig iron in a blast furnace with silicate or aluminosilicate as the main component. When smelting pig iron, the temperature is as high as 150 °C, and GPS is in the molten state [28]. Due to the rapid cooling process (quenching), GPS cannot crystallize; thus, there is no obvious crystal characteristic peak.
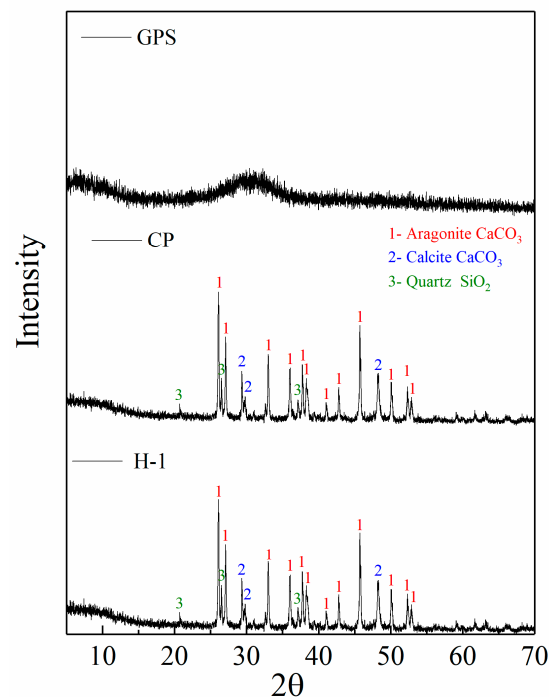

Figure 2. XRD patterns of the GPS, CP and sample H-1.

(2) XRD analysis of CP

The XRD analysis of CP shows aragonite ($CaCO_3$, PDF41-1475) characteristic peaks near 26.2°, 27.2°, 33.1°, 36.2°, 37.9°, 38.6°, 41.2°, 42.8°, 45.8°, 50.2°, 52.4° and 52.9° and the

intensity of the characteristic peaks is high. Meanwhile, there are calcite ($CaCO_3$, PDF47-1743) characteristic peaks near 29.4° and 48.5° and the intensity of the characteristic peaks is also high. The appearance of characteristic peaks of aragonite and calcite indicates that CP contains a large amount of calcareous mineral crystals, which is consistent with the XRF results. Moreover, weak quartz (SiO_2, PDF46-1045) characteristic peaks appear near 20.9°, 26.6° and 36.5°, which indicates that CP also contains a small amount of silicon.

3.3.2. XRD Analysis of GPS Modified Samples

(1) XRD analysis of sample H-1

The XRD analysis of sample H-1 is shown in Figure 2. The characteristic peaks of aragonite, calcite, and quartz are still in sample H-1. No new characteristic peaks were formed, and the intensity of these characteristic peaks have no obvious change compared with CP. This shows that the calcium in sample H-1 does not participate in the polymerization reaction and still exists in an inert form. This is also the main reason why the compressive strength is insufficient. Although liquid sodium silicate contains a large amount of active silicon, it cannot combine with the calcium in sample H-1 to form a hydrated calcium silicate mineral. This is because the calcium in sample H-1 mainly exists as aragonite and calcite minerals and has no polymerization activity. The study in Section 3.1 also explains the low active calcium content in CP despite the high calcium content. Therefore, the lack of reactivity severely inhibits the use of CP alone as alkali-activated materials.

(2) XRD analysis of sample H-3

The XRD analysis of samples H-3, H-7, and H-10 is shown in Figure 3. When 10% GPS was added, the XRD pattern of sample H-3 changed significantly. First, compared with sample H-1, the intensities of aragonite characteristic peaks at 26.2°, 27.2°, 33.1°and 36.2° in sample H-3 are reduced. Moreover, the intensities of calcite characteristic peak at 29.4°and quartz characteristic peak at 26.6°also shows a certain degree of reduction, which shows that the contents of aragonite, calcite, and quartz in sample H-3 are reduced to a certain extent. This is because the incorporation of GPS promotes the synergistic enhancement effect of CP, enhances the polymerization activity of inert calcium in CP, and promotes the formation of polymerization products between calcium and active silicon and aluminum, resulting in the decline of characteristic peaks of aragonite, calcite, and quartz [29].
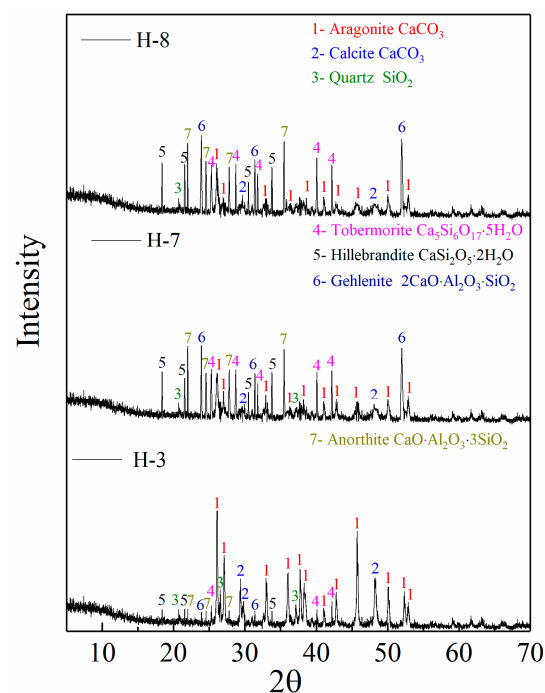

Figure 3. XRD patterns of sample H-3, sample H-7 and sample H-10.

Meanwhile, the characteristic peaks of tobermorite ($Ca_5 \cdot Si_6 O_{17} \cdot 5H_2O$, PDF45-1480) near 25.3°, 40°and 42.1° and hillebrandite ($CaSi_2O_5 \cdot 2H_2O$, PDF42-0538) near 18.4°, 21.6°and 33.8°appeared in sample H-3. Nevertheless, the strength disparity is not obvious, and these two characteristic peaks did not appear in sample H-1. Tobermorite and hillebrandite are all calcium silicate minerals and are considered as hydrated calcium silicate gel, which is the main source of the development of compressive strength in sample H-3. GPS addition improves the reaction activity of calcium in CP and provides a large amount of active silicon for the polymerization environment, which provides favorable conditions for the formation of hydrated calcium silicate [30]. However, since the content of GPS is only 10%, the enhancement effect is still not obvious. The amount of active silicon is still insufficient, resulting in the inadequate formation of hydrated calcium silicate gel. This is the primary reason for the low characteristic peak intensity of tobermorite and hillebrandite, which also explains the less apparent compressive strength enhancement in sample H-3.

Furthermore, the characteristic peaks of gehlenite ($2CaO \cdot Al_2O_3 \cdot SiO_2$, PDF45-1480) near 23.9° and 31.4° and anorthite (CaO. $Al_2O_3 \cdot 2SiO_2$, PDF41-1486) near 22°, 24.5° and 27.8° also appeared in sample H-3. Although the strength is insufficient, these two characteristic peaks did not appear in sample H-1. Gehlenite and anorthite are hydrated calcium aluminosilicate gels synthesized from active calcium, silicon, and aluminum; thus, the compressive strength enhancement effect can be seen in sample H-3. GPS addition brings active silicon and aluminum to the polymerization environment, creating favorable conditions for hydrated calcium silicate aluminate formation [31]. This is why the gehlenite and anorthite crystals appeared in samples H-3. Due to the insufficient GPS amount, the active aluminum content in the polymerization environment is low, resulting in the low strength of the characteristic peak of gehlenite and anorthite. It further substantiates that the formation of hydrated calcium silicoaluminate in sample H-3 is unsatisfactory. Hence, the increase in compressive strength in sample H-3 is not obvious. Therefore, the GPS addition can not only provide active silicon and aluminum, but can also stimulate the activity of calcium in CP. Therefore, the inert calcium can repolymerize to form silicate and aluminosilicate minerals, promoting compressive strength development.

(3) XRD analysis of sample H-7

With the increase in GPS content, the XRD pattern of sample H-7 (50% GPS) further changed dramatically (Figure 3). First, compared with sample H-3 (10% GPS), the intensity of the aragonite characteristic peaks at 26.2°, 27.2°, 33.1°, 36.2°, 37.9°, 41.2°, 42.8°, 45.8°, 50.2° and 52.4° in sample H-7 all further decreased significantly. Moreover, the aragonite characteristic peaks at 38.6° and 52.9° in sample H-7 completely disappeared. Meanwhile, the intensity of the calcite characteristic peaks at 29.6°and 48.5°also decreased significantly, and the peak with the highest calcite strength at 29.4° also disappeared in sample H-7. The decrease or disappearance in the aragonite and calcite characteristic peak indicates that a large amount of inert calcium in sample H-7 is converted into active calcium and a polymerization reaction due to the increase in GPS content. It corroborates the calcium activity in sample H-7 and its participation in increasing the polymerization with GPS content.

More importantly, the tobermorite characteristic peaks at 25.3°, 40° and 42.1° in sample H-7 are significantly improved compared with sample H-3. New tobermorite characteristic peaks appear at 30°and 31.8° in sample H-7, and the intensity is obvious. Similarly, the intensity of hillebrandite characteristic peaks near 18.4°, 21.6°and 33.8° in sample H-7 also increased significantly compared with sample H-3. The characteristic peak intensity of gehlenite near 23.9° and 31.4° also increased significantly, and a new characteristic peak appeared near 52.2° in sample H-7, which was not detected in sample H-3. The intensity of anorthite characteristic peaks near 22°, 24.5°and 27.8° in sample H-7 also significantly improved compared with sample H-3. The increase and appearance of tobermorite, hillebrandite, gehlenite, and anorthite characteristic peak intensity indicate that increasing the GPS amount promotes the polymerization of inert aragonite and calcite minerals to produce calcium silicate and calcium aluminosilicate minerals. Therefore, increasing the amount of GPS can further enhance the activation of inert calcium and

further increase the content of active silicon and aluminum, which promotes the formation of calcium silicate and calcium silicate gel, thereby significantly improving the compressive strength [32].

(4) XRD analysis of sample H-8

When the content of GPS exceeds 50%, the effects of the improvement and activation of CP become less obvious. When the GPS content increases to 60%, although the characteristic peaks of aragonite at 27.2°, 33.1°, 41.2° and 52.4° in sample H-8 (Figure 3) still decrease to a certain extent, the decreasing range is significantly reduced compared with sample H-7. It confirms that the enhancement effect has been significantly reduced. The characteristic peaks of tobermorite (near 40°), hillebrandite (21.6°), and gehlenite (31.4° and 52.2°) in sample H-8 are only slightly enhanced. However, the characteristic peaks of the above minerals from other angles did not increase any more compared with sample H-7. This shows that increasing the GPS content based on 50% cannot significantly improve the formation of calcium silicate and calcium aluminosilicate minerals, which is also the reason for the significant decrease in the compressive strength development rate of sample H-8.

The continuous increase in GPS content inevitably leads to a decrease in CP content, as GPS is used as a substitution material for CP. Although silicon and aluminum content in GPS is much higher than CP, the calcium content in GPS is significantly lower than CP. When the dosage of GPS exceeds 50%, it will inevitably lead to excessive silicon and aluminum in the polymerization environment but in a lack of calcium to participate in polymerization. The lack of calcium will also affect the formation of hydrated calcium silicate and hydrated calcium aluminosilicate gel [33]. This is why the characteristic peaks of calcium silicate and calcium aluminosilicate minerals in sample H-8 are no longer significantly enhanced when increasing the amount of GPS. Therefore, GPS and CP should be used in the optimal ratio (1:1) to realize the optimal activation mode of inert calcium in CP by GPS and the optimal ratio of calcium, silicon, and aluminum in the polymerization environment, to accelerate the polymerization rate and to promote the formation of polymerization products, and finally to significantly improve the compressive strength.

4. Conclusions

In this study, coralline-activated materials were prepared using ball-milled coral powder as cementitious material and coral sand as fine aggregate. XRF and chemical dissolution tests were carried out to determine the content and reactivity of various elements in coral powder. The compressive strength of the developed composites was evaluated at different ages, and the formation and transformation of mineral crystals in coralline-activated samples were further analyzed by XRD.

The following conclusions have been drawn from the obtained results.

(1) Although the calcium content in CP is high, the reaction activity is insufficient, and the content of silicon and aluminum is unsatisfactory, which seriously affects the polymerization activity of CP and the formation of polymerization products. The addition of GPS can improve the reactivity of calcium in CP and the defect of insufficient silicon and aluminum content in CP.

(2) With the increase in GPS content (0% to 50%), the compressive strength of samples H-3 to H-7 increases significantly, but when the GPS content is higher than 50%, the growth range decreases significantly.

(3) The incorporation of GPS makes up for the deficiency of silicon and aluminum in CP. It improves the polymerization activity, which promotes the transformation of inert aragonite and calcite mineral crystals in CP into high-strength polymerization products. However, when the content of GPS exceeds 50%, silicon and aluminum content in the polymerization reaction environment is too high, while the calcium content is reduced. It affects the formation of polymerization products and cannot further significantly improve the strength of the samples.

References

1. Shen, Y.; Feng, Z.; Qi, W.; Ma, Y.; Liu, H. Sedimentary characteristics of coral mud in the South China Sea during the reclamation process. *Geo-Mar. Lett.* **2019**, *39*, 417–425. [CrossRef]
2. Ye, J.; Shan, J.; Zhou, H.; Yan, N. Numerical modelling of the wave interaction with revetment breakwater built on reclaimed coral reef islands in the South China Sea-Experimental verification. *Ocean Eng.* **2021**, *235*, 109325. [CrossRef]
3. Liu, J.; Ou, Z.; Peng, W.; Guo, T.; Deng, W.; Chen, Y. Literature Review of Coral Concrete. *Arab. J. Sci. Eng.* **2018**, *43*, 1529–1541. [CrossRef]
4. Chu, Y.; Wang, A.; Zhu, Y.; Wang, H.; Liu, K.; Ma, R.; Guo, L.; Sun, D. Enhancing the performance of basic magnesium sulfate cement-based coral aggregate concrete through gradient composite design technology. *Compos. Part B* **2021**, *227*, 109382. [CrossRef]
5. Wang, X.; Yu, R.; Shui, Z.; Song, Q.; Zhang, Z. Mix design and characteristics evaluation of an eco-friendly UltraHigh Performance Concrete incorporating recycled coral based materials. *J. Clean. Prod.* **2017**, *165*, 70–80. [CrossRef]
6. Qin, Q.; Meng, Q.; Yang, H.; Wu, W. Study of the anti-abrasion performance and mechanism of coral reef sand concrete. *Constr. Build. Mater.* **2021**, *291*, 123263. [CrossRef]
7. Liu, J.; Ju, B.; Xie, W.; Zhou, T.; Xiao, H.; Dong, S.; Yang, W. Evaluation of the Effects of Surface Treatment Methods on the Properties of Coral Aggregate and Concrete. *Materials* **2021**, *14*, 6784. [CrossRef]
8. Ma, L.; Li, Z.; Liu, J.; Duan, L.; Wu, J. Mechanical properties of coral concrete subjected to uniaxial dynamic compression. *Constr. Build. Mater.* **2019**, *199*, 244–255. [CrossRef]
9. Liu, J.; Ju, B.; Xie, W.; Yu, H.; Xiao, H.; Dong, S.; Yang, W. Design and Evaluation of an Ultrahigh-Strength Coral Aggregate Concrete for Maritime and Reef Engineering. *Materials* **2021**, *14*, 5871. [CrossRef]
10. Wang, A.; Lyu, B.; Zhang, Z.; Liu, K.; Xu, H.; Sun, D. The development of coral concretes and their upgrading technologies:A critical review. *Constr. Build. Mater.* **2018**, *187*, 1004–1019. [CrossRef]
11. Provis, J.L.; Palomo, A.; Shi, C. Advances in understanding alkali-activated materials. *Cem. Concr. Res.* **2015**, *78*, 110–125. [CrossRef]
12. Shi, C.; Fernández-Jiménez, A.; Palomo, A. New cements for the 21st century: The pursuit of an alternative to Portland cement. *Cem. Concr. Res.* **2011**, *41*, 750–763. [CrossRef]
13. Puertas, F.; González-Fonteboa, B.; González-Taboada, I.; Alonso, M.M.; Torres-Carrasco, M.; Rojo, G.; Martínez-Abella, F. Alkali-activated slag concrete: Fresh and hardened behavior. *Cem. Concr. Compos.* **2018**, *85*, 22–31. [CrossRef]
14. Huang, G.; Yang, K.; Chen, L.; Lu, Z.; Sun, Y.; Zhang, X.; Feng, Y.; Ji, Y.; Xu, Z. Use of pretreatment to prevent expansion and foaming in high-performance MSWI bottom ash alkali-activated mortars. *Constr. Build. Mater.* **2020**, *245*, 118471. [CrossRef]
15. Luukkonen, T.; Abdollahnejad, Z.; Yliniemi, J.; Kinnunen, P.; Illikainen, M. One-part alkali-activated materials: A review. *Cem. Concr. Res.* **2018**, *103*, 21–34. [CrossRef]
16. *GB/T176-2017*; Methods for Chemical Analysis of Cement. AQSIQ: Beijing, China, 2017.
17. Shi, Z.; Shi, C.; Zhang, J.; Wan, S.; Zhang, Z.; Ou, Z. Alkali-silica reaction in waterglass-activated slag mortars incorporating fly ash and metakaolin. *Cem. Concr. Res.* **2018**, *108*, 10–19. [CrossRef]
18. Huang, G.; Ji, Y.; Li, J.; Zhang, L.; Liu, X.; Liu, B. Effect of activated silica on polymerization mechanism and strength development of MSWI bottom ash alkali-activated mortars. *Constr. Build. Mater.* **2019**, *201*, 90–99. [CrossRef]
19. Bergold, S.; Goetz-Neunhoeffer, F.; Neubauer, J. Interaction of silicate and aluminate reaction in a synthetic cement system: Implications for the process of alite hydration. *Cem. Concr. Res.* **2017**, *93*, 32–44. [CrossRef]
20. Huang, G.; Yang, K.; Sun, Y.; Lu, Z.; Zhang, X.; Zuo, L.; Feng, Y.; Qian, R.; Qi, Y.; Ji, Y.; et al. Influence of NaOH content on the alkali conversion mechanism in MSWI bottom ash alkali-activated mortars. *Constr. Build. Mater.* **2020**, *248*, 118582. [CrossRef]
21. Maraghechi, H.; Rajabipour, F.; Pantano, C.G.; Burgos, W.D. Effect of calcium on dissolution and precipitation reactions of amorphous silica at high alkalinity. *Cem. Concr. Res.* **2016**, *87*, 1–13. [CrossRef]

22. Huang, G.; Ji, Y.; Zhang, L.; Li, J.; Hou, Z. The influence of curing methods on the strength of MSWI bottom ash-based alkali-activated mortars: The role of leaching of OH− and free alkali. *Constr. Build. Mater.* **2018**, *186*, 978–985. [CrossRef]
23. Huang, G.; Ji, Y.; Li, J.; Hou, Z.; Dong, Z. Improving strength of calcinated coal gangue geo-polymer mortars via increasing calcium content. *Constr. Build. Mater.* **2018**, *166*, 760–768. [CrossRef]
24. Angulo-Ramírez, D.E.; de Gutiérrez, R.M.; Puertas, F. Alkali-activated Portland blast-furnace slag cement: Mechanical properties and hydration. *Constr. Build. Mater.* **2017**, *140*, 119–128. [CrossRef]
25. Li, C.; Sun, H.; Li, L. A review: The comparison between alkali-activated slag (Si+Ca) and metakaolin (Si+Al) cements. *Cem. Concr. Res.* **2010**, *40*, 1341–1349. [CrossRef]
26. Huang, G.; Ji, Y.; Hou, J.L.Z.; Jin, C. Use of slaked lime and Portland cement to improve the resistance of MSWI bottom ash-GGBFS geopolymer concrete against carbonation. *Constr. Build. Mater.* **2018**, *166*, 290–300. [CrossRef]
27. Huang, G.; Ji, Y.; Zhang, L.; Li, J.; Hou, Z. Advances in Understanding and Analyzing the Anti-diffusion Behavior in Complete Carbonation Zone of MSWI Bottom Ash-based Alkali-activated Concrete. *Constr. Build. Mater.* **2018**, *186*, 1072–1081. [CrossRef]
28. Huang, G.; Li, Y.; Zhang, Y.; Zhu, J.; Li, D.; Wang, B. Effect of Sodium Hydroxide, Liquid Sodium Silicate, Calcium Hydroxide, and Slag on the Mechanical Properties and Mineral Crystal Structure Evolution of Polymer Materials. *Crystals* **2021**, *11*, 1586. [CrossRef]
29. Huang, G.; Yuan, L.; Ji, Y.; Liu, B.; Xu, Z. Cooperative action and compatibility between Portland cement and MSWI bottom ash alkali-activated double gel system materials. *Constr. Build. Mater.* **2019**, *209*, 445–453. [CrossRef]
30. Huang, G.; Ji, Y.; Zhang, l.; Hou, Z.; Zhang, L.; Wu, S. Influence of calcium content on structure and strength of MSWI bottom ash-based geopolymer. *Mag. Concr. Res.* **2019**, *71*, 362–372. [CrossRef]
31. Swanton, S.W.; Heath, T.G.; Clacher, A. Leaching behaviour of low Ca:Si ratio CaO–SiO$_2$–H2O systems. *Cem. Concr. Res.* **2016**, *88*, 82–95. [CrossRef]
32. Puertas, F.; Palacios, M.; Manzano, H.; Dolado, J.S.; Rico, A.; Rodríguez, J. A model for the C-A-S-H gel formed in alkali-activated slag cements. *J. Eur. Ceram. Soc.* **2011**, *31*, 2043–2056. [CrossRef]
33. L'Hôpital, E.; Lothenbach, B.; Scrivener, K.; Kulik, D. Alkali uptake in calcium alumina silicate hydrate (C-A-S-H). *Cem. Concr. Res.* **2016**, *85*, 122–136. [CrossRef]